Frontiers in Heat and Mass Transfer (FHMT), 19, 2 (2022)
DOI: 10.5098/hmt.19.2

Global Digital Central
ISSN: 2151-8629

Frontiers in Heat and Mass Transfer

Available at www.ThermalFluidsCentral.org

AN ULTIMATE SOLUTION TO PHASING OUT FOSSIL FUELS – PART II: AIR-WATER THERMAL POWER PLANTS FOR UTILITY-SCALE POWER PRODUCTION AT LOW TEMPERATURES

Yiding Cao

Department of Mechanical and Materials Engineering, Florida International University, Miami, FL 33174, USA

ABSTRACT

This paper introduces a novel air-water thermal power plant working at low temperatures and employing hot water as a heat-supply fluid to produce utility-scale power with high second-law efficiency. The air-water power plant uses both air and water as working fluids and employs a direct-contact mass and heat transfer packing to facilitate latent heat (in terms of vapor) and sensible heat transfer from the hot water to moist air for expansion in a gas turbine to produce power. A cycle analysis indicates that with a heat source temperature of around 100ºC, the power plant could achieve a power capacity of more than 300 MW, matching the power capacity of fossil-fuel-based power plants, with a thermal-to-mechanical conversion efficiency above 16%. The power plant could also work in summer involving high temperature/high humidity ambient air by using a chiller to cool the power-plant intake air, the inlet air of the compressor system, or the air in a compressor intercooler. In addition to power production, the power plant could supply hot water for heat or water users. This power plant employs completely clean working fluids of air and water, operates at low temperature and pressure, and can use renewable energy such as solar energy and geothermal energy, as well as heat from other sources including industrial waste heat, to produce utility-scale power with low costs. Combined with hot-water thermal-energy storage systems, the power plant introduced could use renewable energy sources to produce dispatchable power reliably for phasing out most fossil fuels used today and becoming a backbone of national power grids to combat global warming and reduce pollution.

Keywords: *Thermal Power Plant, Renewable Energy, Direct-Contact Heat and Mass Transfer, Regenerator Condenser, Chiller Cooling*

1. INTRODUCTION

Thermal power plants that could enable the use of the vast amount of thermal energy resources at low or medium temperatures to generate electricity could have a significant impact on the advancement of renewable energy. Cao (2022a) demonstrated the concept of utility-scale underground hot-water storage facilities in conjunction with thermal power plants, which could have the potential to displace more than 80% of the global fossil fuel being used today. However, economic feasibility of the storage systems is very sensitive to their temperature and pressure, and a favorable temperature range was shown to be near or slightly above 100ºC, more specifically in the low-mid temperature range between 90 to 150ºC. If the water temperature is significantly above this range, the costs of the hot-water storage system could increase exponentially. Also, heat acquisition by the water through solar collectors or geothermal energy favors a lower temperature. As the solar collector temperature is increased, the collector efficiency could decrease from around 80% to below 50%. For a higher temperature above 200ºC, concentrating solar collectors may have to be employed, which not only increases the costs of the solar acquisition significantly but also would fail to collect the diffuse component of the solar flux, which is generally 25% to 50% of the total solar flux.

Thermal power plants that could generate power at a lower temperature range are also essential to geothermal power production. According to U.S. DOE Energy Efficiency and Renewable Energy (EERE, 2022), geothermal energy resources below 300°F (149ºC) would represent the most common geothermal resource. One of the biggest challenges for geothermal exploration is the significant cost of drilling deep wells for a higher heat source temperature, which may require extensive drilling at depths of 3,000 to 5,000 m depending on the project geology. As the depth of geothermal drilling increases, the cost of drilling would increase exponentially, which may render the project economically infeasible.

Conventional steam-turbine-based power plants that are commonly used in coal-burning vapor power plants and nuclear power plants may be a candidate for solar and geothermal applications, and steam-turbine power plants have been used to generate power using dry steam from geysers. However, according to EERE, the most common geothermal power applications are flash steam power plants, and their uses are limited to the heat source temperature higher than 360°F (182°C). For this reason, binary cycle geothermal power plants are being used for heat source temperatures below 200ºC. In a binary-cycle-based geothermal power plant, heat from the geothermal liquid is transferred to a second fluid that has a boiling temperature lower than water through a heat exchanger (EERE, 2022). The second fluid, generally isobutane, pentane, or ammonia under highly pressurized conditions, receives heat from the geothermal liquid through vaporization. The vapor generated in the heat exchanger is ducted to an expander to produce power. The exhaust flow of the second fluid out of the expander is condensed through a closed-loop condenser and returns to the geothermal liquid heat exchanger to complete the cycle. Modular systems with unit capacities ranging from 1 to 3 MW are normally used (Salameh, 2014). The high pressure and closed-loop mean that the system may incur high costs. It should be pointed out that isobutane, pentane, and ammonia are all highly hazardous substances. Their uses

on a limited scale may be acceptable, but large-scale uses may cause significant health and environment-related consequences due to the potential leakage out of the power plant under highly pressurized conditions.

Refrigerants such as R-134a, R-123, and R245fa are popular working fluids for many other Organic Rankine Cycle (ORC) systems (Quoilin et al., 2011). However, refrigerants generally have a very low specific vapor volume (or high vapor density). Since the turbine power production is scaled to the product of specific vapor volume and the pressure drop through the expansion in a turbine, the power production per unit mass flow rate is very limited under a given pressure drop. As a result, the power capacity of the ORC power plants using refrigerants as the working fluid is generally low, on the order of kW, which may be unable to meet the requirement for utility-scale power production.

2. THE CONCEPT OF AIR-WATER THERMAL POWER PLANTS

Air and water are the most essential natural fluids on the earth and their mutual interactions as well as with soil and other natural resources sustain life on the earth. They are also the working fluids of power plants and engines since the industrial revolutions more than 250 years ago. Water is the working fluid of steam engines and vapor power plants burning fossil fuels, as well as nuclear power plants, while air is the working fluid of internal combustion (IC) engines and aircraft engines as well as industrial gas turbine power plants. In terms of core operational thermodynamic cycles, the air is the exclusive working fluid of IC engines and gas-turbine-based power plants while water is excluded. On the other hand, water is the working fluid of steam engines and vapor power plants while air is excluded (Bathie, 1996; Moran et al., 2011). For example, in a steam engine or vapor power plant, any meaningful accumulation of air is not tolerable and must be removed through a vacuum pump system. However, in an analogy to positive electric charge and negative electric charge and from a philosophic point of view, the air and water may form a couple; one is the positive fluid while the other is the negative fluid and vice versa. Their intimate interplay is essential to lives and ecosystems on the earth. For example, their interaction facilities the water cycle in meteorology (NOAA, 2022) which has significant importance on the climate systems and ecosystems. It is believed that their interactions could also enable a new power plant by using renewable energy sources and working at a sufficiently low temperature to achieve utility-scale power production without involving hazardous working fluids (Cao, 2022b).

In an air-water power plant of this paper, air or air-vapor mixture is an energy-receiving fluid while hot water is a heat-supply fluid to enable power production through an expander such as a turbine. The hot water may be preferably a liquid, but it could also be a liquid-vapor two-phase mixture or a superheated vapor. The energy acquisition by the working fluid may be in a form of combined latent and sensible heat in terms of the hot water evaporation and vapor addition into the air or air-vapor mixture flow in a direct-contact mass and heat transfer exchanger or packing. The vapor along with the dry air would then produce power in an expander such as a turbine. Due to the high latent heat of the vapor, on the order of 2200 kJ/kg, even if the sensible heat acquisition may be limited, the total energy acquisition may be high to produce enough power. Since the dry-air flow stream is essential a constant throughout the packing and turbine, the power production capacity of the turbine may be directly linked to the amount of vapor content per unit kg of dry air in the air-vapor mixture flow stream into the turbine. A parameter to measure the vapor content or the latent heat level in moist air or air-vapor mixture is the humidity ratio (or specific humidity) W in kg of vapor mass per kg of dry air, and the related air-vapor mixture enthalpy at the inlet of a turbine, in kJ per kg of dry air, can be approximated by the following relation (McQuiston, 2005).

$$h_i = c_{pa} \times t + W \times (h_{fg} + c_{pv} \times t) \quad (1)$$

where t is the temperature in degree ^oC, c_{pa} is the specific heat of dry air, h_{fg} is the water latent heat of vaporization at 0^oC, and c_{pv} is the corresponding vapor specific heat. It is well known that in a thermal power plant, the enthalpy of the working fluid at the inlet of a turbine would determine the power production capacity of the turbine under given turbine outlet conditions (Moran et al., 2011), as shown by Eq. (2) below, after the effects of the kinetic and potential energies, as well as the strayed heat loss from the turbine, are neglected:

$$w_t = h_i - h_o \quad (2)$$

where w_t is the work developed by the turbine, h_i is the enthalpy at the turbine inlet, and h_o is the enthalpy at the turbine outlet. For the air-water power plant of this paper, for convenience, all three terms in Eq. (2) would have a unit of kJ/kg dry air. The inlet enthalpy from Eq. (1) would represent the total energy content of the air-vapor mixture which subsequently determines the power production capacity of the power plant. It is clear from Eq. (1) that the total enthalpy is largely determined by the humidity ratio W, as the first term on the right side of Eq. (1), which represents the sensible heat of dry air, is rather small for the present low-temperature power plants. In contrast, for a conventional fossil-fuel-based gas turbine power plant, the second term on the right side of Eq. (1) is essentially close to zero, and the sensible heat represented by the first term is the contributor to the turbine-inlet enthalpy. The temperature in the first term often may need to be more than 1500^oC through the combustion of fossil fuels to attain sufficient sensible heat for high turbine power production.

Referring to Eq. (1), the saturated humidity ratio under given thermodynamics conditions would represent the maximum amount of vapor that the air-vapor mixture could accommodate, which would then determine the maximum thermal energy content of the mixture at the turbine inlet as well as the maximum power capacity of the turbine under given turbine inlet temperature and outlet conditions. The following relation can be used to calculate the saturated humidity ratio (McQuiston, 2005; Moran et al., 2011) with sufficiently high accuracy:

$$W_s = 0.622 \frac{p_s(t)}{(p_t - p_s(t))} \quad (3)$$

where p_s is the saturation pressure corresponding to the temperature of the air-vapor mixture and p_t is the total or system pressure of the mixture. Table 1 shows the saturated humidity ratio, the latent heat content, sensible heat content, and the latent heat share under some air-water mixture conditions in terms of temperature and total pressure, wherein the latent heat content is defined as the thermal energy associated with the vapor component.

Table 1: Latent heat potential of the air-vapor mixture at some given temperature and total pressure

t (°C)	p_s (bar)	p_t (bar)	W_s (vapor/dry-air)	Latent heat (kJ/kg dry air)	Sensible heat (kJ/kg dry air)	Latent heat share (%)
126	2.383	3.03	2.290	6305.1	126.0	98.0
116.2	1.753	2.53	1.412	3881.9	116.2	97.1
106.3	1.267	2.02	1.045	2822.5	106.3	96.4
96.6	0.896	1.01	4.91	13176.1	96.6	99.3
86.9	0.621	1.52	0.432	1155.6	86.9	93.0
40 (for cooling tower applications)	0.0738	1.01	0.0491	126.7	40	76.0

As can be seen from Table 1, within a temperature range of 86.9^oC to 126^oC, the latent heat content in the air-vapor mixture is dominant. For example, at a temperature of 116.2^oC, the latent heat component in the mixture is more than 97% with almost negligible sensible heat contribution. The results in the table also show that although the operating temperature has a dominant effect on the saturation humidity

ratio, a lower system pressure or total pressure may significantly improve the humidity ratio. For example, at a temperature of 96.6°C and a total pressure of 1.01 bar, the saturation humidity ratio has a value of about 4.91, much higher than that at a higher temperature of 126°C and a higher total pressure of 3.03 bar. Table 1 also shows a case of a cooling tower application with an upper-end temperature of 40°C. In cooling tower applications, the sole objective is to cool the water down to close to the ambient temperature through water evaporation into the air, and the air conditions in the tower are not an interest of the operation. Still, even though the magnitude of the latent heat component in the moist air is rather small due to the low temperature, its share in the total energy content of the moist air is more than 75%.

3. FIRST EMBODIMENT OF AIR-WATER THERMAL POWER PLANTS

Figure 1 illustrates schematically an air-water thermal power plant unit in terms of an axial turbine of a generally circular cross-section using hot water as a heat-supply fluid with frontal air compression (Cao. 2022b).

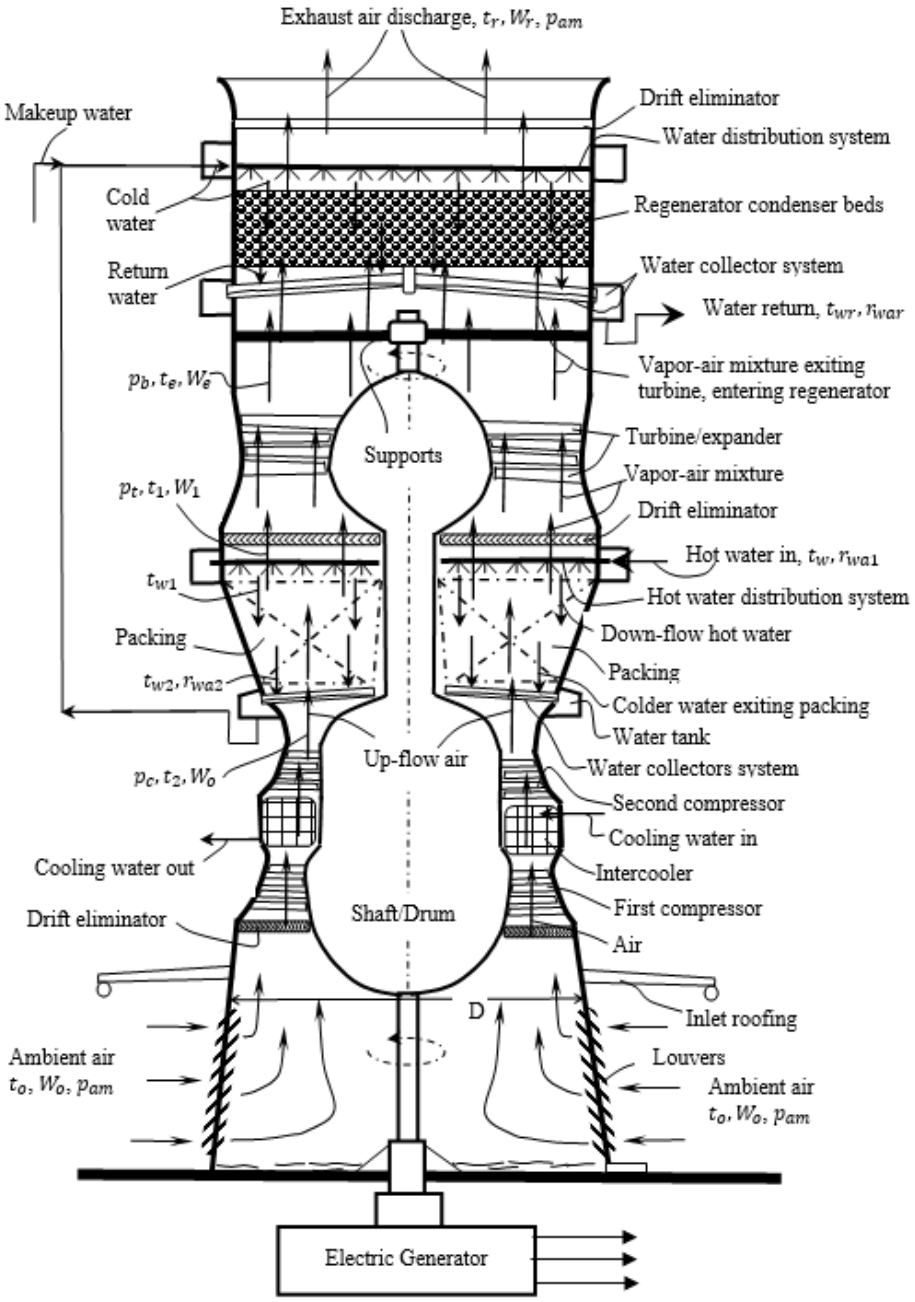

Fig. 1: A schematic vertical sectional view of an air-water power plant unit employing a packing for working-fluid energy acquisition before expansion in a turbine.

Global Digital Central
ISSN: 2151-8629

Because of the advantageous open-cycle, simpler structure, and quick startup of the gas turbine cycle over the closed-cycle of vapor power plants, a gas turbine power platform is adopted for the first embodiment of the air-water power plant. Referring to Fig. 1 and starting from the bottom of the power plant, ambient moist air at t_o and W_o as well as pressure p_{am} is induced into the power plant through an air inlet section with louvers. The air converges and flows upward to the inlet of the first compressor of a compressor system. A drift eliminator may be installed before the inlet of the compressor to prevent liquid or solid particles from entering the compressor. An inlet roofing may be disposed around the casing of the power plant, as shown in the figure, for a similar purpose, particularly for storming or snowing weather conditions. If the combined functions of inlet roofing and louvers are sufficiently effective to prevent liquid or solid particles from entering the compressor, the drift eliminator at the inlet of the compressor may not be necessary.

The airstream enters the first compressor of the compressor system, which may include at least two compressors and at least an intercooler, and is compressed to a higher pressure and higher temperature. Then the air flows through an intercooler and may be cooled back to near its inlet temperature to the first compressor. As shown in Fig. 1, cooling water for the intercooler enters the intercooler through an upper section and exits the intercooler through a lower section. Because of the preferred low-temperature operational characteristics of the air-water power plant, it is essential to adequately cool the air through the intercooler and maintain a lower temperature at the outlet of the compressor system. The intercooler would also reduce the compressor power consumption and increase the energy recovery from a regenerator which will be described later in this paper. The intercooler could be any suitable type of heat exchanger including counterflow and crossflow types, but a particular type of microchannel heat exchanger may have the advantage for the present application for air temperature reduction and lower pressure drop across the intercooler. The cooled air continues its flow path after the intercooler and enters the second compressor. The compressed air stream with a further increased pressure leaves the second compressor with p_c, t_2, W_o, as shown on the left side of the figure. Although Fig.1 shows only one intercooler and two compressors, more than one intercooler and more than two compressors may be installed.

Upon leaving the compressor system, the compressed air enters a packing to acquire latent and sensible heat from counterflowing hot water to raise its vapor content and temperature, which essentially becomes an air-vapor mixture. The packing, fill, or packed bed herein is a direct-contact heat and mass exchanger between hot water and air-vapor mixture. In this paper, moist air and air-vapor mixture are interchangeably used. However, the term moist air may signify that vapor content in the air is relatively small, while the air-vapor mixture may signify that the vapor content in the mixture is significant. Through the intimate contacts between the down-flowing hot water and up-flowing colder air-vapor mixture, combined mass and heat transfer takes place from the hot water to the air-vapor mixture at the interfaces between the hot water and air-vapor mixture. Hot water vaporizes at the interface and enters the air-vapor mixture stream due to higher vapor pressure at the interface than the partial vapor pressure in the air-vapor mixture. The packing is essentially a system of baffles to slow down the progress of the hot water and maximize the contact between the hot water and the air-vapor mixture (Hill et al., 1990). It may also increase the contact surface area between the hot water films and the air-vapor mixture as well as minimizes the thickness of hot water films. Another packing design objective is to minimize the pressure drop of the air-vapor mixture across the packing. Figure 2 is a flow-pattern conceptual illustration of a local area in the packing, wherein the upward air-mixture flow, the downward hot water film flow, vapor mass flux from the liquid-vapor interface entering the air-vapor mixture, and the solid matrix of the packing are schematically shown. However, the sensible heat transfer from the liquid film to the air-vapor mixture is not shown, which raises the temperature of the air-vapor mixture from the bottom to the top of the packing. It should be emphasized that the conceptual illustration in Fig. 2 may not reflect the real configuration of the flow passages and packing solid matrix, which could be characterized as complex, tortuous, and random to benefit the intensity of the mass and heat transfer.

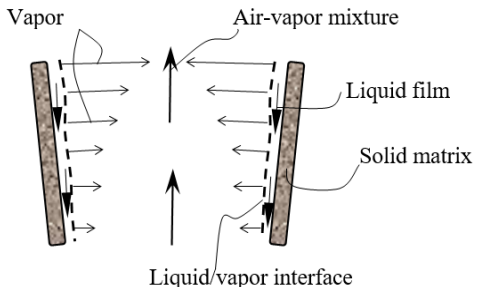

Fig. 2: A schematic, conceptual illustration of the flow pattern in a local area of the packing.

Packings and their theories and applications for cooling towers have been described in detail by Hill et al. (1990), Hewitt et al. (1994), and others. The packing for the air-water power plant of this paper may have a similar configuration found in cooling towers for wet cooling the coolants of power and air-conditioning systems, but with a different objective. In the cooling tower applications, the objective of using a packing is to cool a water flow as low as possible to be used as the condenser coolant of a power plant or a chiller for an air conditioning (A/C) application (McQuiston et al., 2005 and Moran et al., 2011), while the thermal conditions of the moist air that is discharged into the ambient is not an interest. On the other hand, the objective of the present application through the packing is to increase the energy content of the air-vapor mixture through the increase of its vapor contents and temperature, so that the energy contents of the mixture can be used to generate power through a turbine or other expanders.

Referring to Fig. 1 again, after the energy acquisition in the packing, the air-vapor mixture exits the packing with increased humidity ratio and temperature, W_1 and t_1, as shown on the left side of the figure. Upon passing through a drift eliminator to remove liquid droplets, the air-vapor mixture is ducted into a turbine to produce power through expansion. In the illustration in Fig. 1, the turbine, compressors, and electric generator may be linked through a shaft/drum. A portion of the power generated by the turbine is used to drive the compressor system and the remaining power may be used to generate electricity through the electric generator, as shown near the bottom of Fig. 1. A starter and other necessary systems may also be disposed but are not shown in the figure. After the expansion and converting some of the thermal energy content into power, the air-vapor mixture exits the turbine with reduced pressure p_b , temperature t_e, and humidity ratio W_e, wherein p_b is the pressure at the outlet of the turbine or backpressure, as shown in Fig. 1. But the air/vapor mixture exiting the turbine may still contain a large amount of unused thermal energy, particularly in terms of vapor content in the mixture, and direct discharge into the ambient would seriously affect the thermal efficiency of the power plant. Therefore, a regenerator condenser is employed to recover a significant amount of the energy from the mixture, and the air-vapor mixture would continue its flow path to enter the regenerator. However, before completing the description of the air-vapor mixture process, let's switch the attention to the hot water as the heat-supply fluid of the power plant unit.

Referring to packing in the middle section of Fig. 1, hot water, as a heat-supply fluid, at a temperature t_w, enters the power plant through a hot water distribution system on top of the packing. The hot water may be delivered from a storage system or directly from a heat source. The heat source may be, but is not limited to, solar energy, geothermal energy, or industrial waste heat. Since the dry air mass may be constant from the inlet to the outlet of the power plant, similar to the cooling

Global Digital Central
ISSN: 2151-8629

tower, the power plant analysis herein is based on the unit mass of the dry air. Therefore, the mass flow of the hot water at the inlet of the power plant is measured in kg of water per kg of dry air, $r_{wa1} = \dot{m}_{w1}/\dot{m}_{air}$, as shown in the figure. Because some liquid may flash into vapor through the hot water distribution system, the actual temperature of the hot water entering the packing from the top would be t_{w1}. Through the mass and heat transfer as well as counterflow arrangement, the hot water may impart a significant amount of its thermal energy to the air-vapor mixture, accompanied by a significant reduction in the water temperature. The water with a reduced temperature of t_{w2} and a lower water mass flow rate of r_{wa2} exits the packing at the packing bottom. Notice that r_{wa2} is less than r_{wa1} because in the packing some of the water has been vaporized and the generated vapor has joined the up-flowing air-vapor mixture.

The colder water out of the packing is collected by a collector system comprising arrays of longitudinal collectors that may have a pan or bow-shaped cross-section and a peripheral water tank. The collector system would extend radially and would incline downwardly from the power plant central region to the plant casing, so the gravitational force is unitized to drive the water to the peripheral water tank. A sectional view of the collector arrangement is schematically shown in Fig. 3. Referring to Fig. 3, a plurality of circumferential rows of collector elements of a pan or bow-shaped cross-section is staggered in the direction of the water flow to capture and collect the water out of the packing. The width of the collector elements may also increase radially because of the increased circumference with increased radius. The arrangement of the collector elements would also aim to reduce the pressure loss of the moist air across the collector to enter the packing.

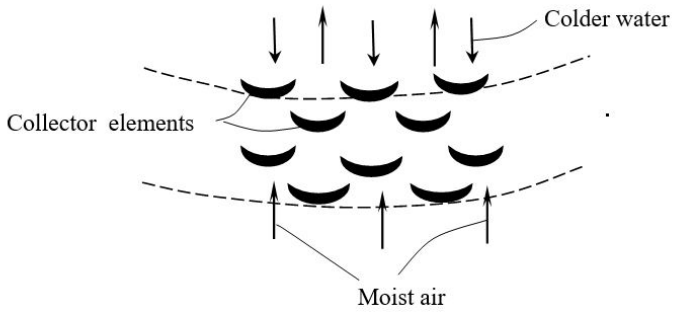

Fig. 3: A schematic, sectional view of the water collector system as shown in Fig. 1.

As mentioned earlier in this paper, the water exiting the packing and being collected by the collector system may have a significantly reduced temperature and associated energy content because of the mass and heat transfer in the packing. The water could be directly pumped from the peripheral water tank to a storage system to be heat-recharged or directly sent to a heat source, such as solar collectors or other heat sources, for recharge. However, if the water is pumped from the water tank to a regenerator to recover a significant amount of energy from the air-vapor mixture exiting the turbine, a lot of energy could be saved.

The regenerator, as shown near the top of the power plant in Fig. 1, would be a counter-flow, direct-contact condenser with a packed bed, wherein the colder water exiting the packing is pumped from the water tank at the bottom of the packing to a water distribution system on top of the regenerator (see upper left of Fig. 1). The packed bed creates intimate contact between the colder, down-flowing water and up-flowing hotter air-vapor mixture exiting the turbine and entering the regenerator from the bottom of the bed, which effectively condenses vapor in the air-vapor mixture and heats the water through the condensation released heat. The condensate would join the downflowing water flow stream and increase the water mass flow rate from the top to the bottom of the regenerator. Compared to a non-direct contact condenser with walls separating the vapor from cooling water flow, the direct contact condenser with the bed could have hugely increased condensation efficiency because of the drastically increased condensation surface area between the vapor and cooling water and minimized thermal resistance between the direct contacting vapor and cooling water. The direct-contact condenser could condense nearly all the vapor with limited bed height, and the final temperature of the water would depend on the energy balance between the inlet vapor flow and the inlet water flow (Hewitt et al., 1994). The exiting temperature of the water at the bottom of the bed could be very close to the inlet vapor temperature when the total inlet vapor flow energy content is higher than the maximum energy acquisition potential of the inlet water flow. After recovering a substantial amount of energy from the air-vapor mixture through the regenerator, the water, with an increased temperature of t_{wr} and mass flow rate of r_{war}, exits the regenerator and is collected by a water collection system of the regenerator. The collected water may be pumped from the peripheral water collection tank to a storage facility or directly to a heat source to be thermally recharged. The water flow rate out of the regenerator may not be the same as that of the hot water at the inlet of the power plant before the turbine. However, some makeup water may be added to the top of the regenerator, as shown in Fig. 1 near the top of the power plant. As a result, the water flow rate per kg of dry air out of the power plant r_{war} may approach r_{wa1}, the hot water flow rate entering the power plant, for power cycle considerations.

On the air-vapor mixture side, the mixture enters the regenerator from the bottom of the regenerator condenser with t_e, W_e, and leaves the regenerator with significantly reduced temperature and vapor content, t_r, W_r. After passing through a drift eliminator, the air-vapor flow stream out of the regenerator is discharged into the ambient as exhaust. However, the exhaust may still contain a significant amount of water vapor and heat, and a water or heat recovery unit may be added to recover as much water or heat as possible before the exhaust airflow stream is discharged into the ambient. The water or heat recovery is not included in Fig. 1 because of its emphasis on power production, but it will be discussed in the following of this paper.

To further illustrate the air-water power plant as shown in Fig. 1, a flow diagram demonstrating the operational principle of the power plant is shown in Fig. 4. A water or heat recovery unit is also added after the regenerator condenser. The water or heat recovery opens the door for the dual use of power and heat, as the recovered water and heat may be delivered for various uses, such as, but not limited to, domestic hot water, home heating, and industrial uses. In many cases, an open-cycle power plant may be preferred. However, this does not exclude the operation of a closed-cycle power plant. Additionally, thermodynamics cycle analyses are often based on the concept of a closed cycle even if the real operation is the open cycle. For these reasons, the operation as shown in Fig. 4 may be treated as a closed cycle. As shown by the dashed lines; after further removing some moisture and reducing the temperature, the exhaust flow may return to the inlet of the compressor system as the ambient air. It should also be mentioned that in many real situations, the water or heat recovery unit in Fig. 4 may be combined with the regenerator condenser.

In the air-water power plant, both air and water are core components of the working fluids, and for this reason, the thermodynamic cycles for both air-vapor mixture and hot water are used to illustrate the working principle of the power plant. Figure 5a shows a thermodynamic cycle for the air-vapor mixture in terms of a *t-s* diagram with certain idealizations. As mentioned before, the dry-air mass flow rate through the power plant may be unchanged, and the cycle would be conveniently illustrated based on the mass of the air-vapor mixture per kg of dry air. At the inlet of a compression system that may include at least one intercooler, the temperature of the ambient moist air is t_o, the mass of the vapor in the ambient air is W_o (the humidity ratio), and the pressure is p_{am}. The ambient moist air mass on the basis of per kg dry air would be $1+W_o$. The moist air is compressed by the compression system (marked as compression) to a higher pressure p_c with the input of an amount of mechanical work, w_{com}.

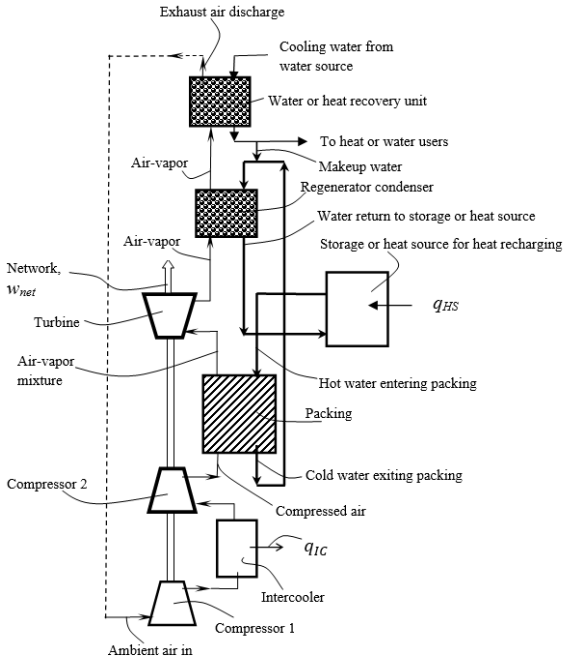

Fig. 4: A flow diagram demonstrating the operation principle of the power plant as shown in Fig. 1, including a water/heat recovery unit for water or heat usage.

The compressed moist air leaves the compression system at t_2 and $1+W_o$, and enters a direct-contact packing (heat and mass exchanger), wherein the moist air simultaneously receives both vapor and heat from a hot-water flow stream. The air-vapor mixture leaves the packing with an increased temperature and humidity ratio, t_1, W_1, along with a pressure of p_t that may be close to p_c as the pressure drop through the packing is generally small. Vapor addition to the air-vapor mixture on the basis of 1 kg dry air would be $W_1 - W_o$, as marked in Fig. 5a. The air-vapor mixture then enters a turbine to develop an amount of shaft work, w_{tur}, and leaves the turbine with the condition of reduced temperature and pressure, represented by t_e, p_b. The vapor content represented by W_e may also be lower than W_1 due to some vapor condensation through the expansion in the turbine. The air-vapor mixture further reduces its energy content in a regenerator condenser, where its vapor content is significantly reduced through vapor mass condensation and heat transfer to the colder water entering the regenerator from the top of the regenerator. At the outlet of the regenerator, the air-vapor mixture has a reduced vapor content of W_r along with a reduced temperature of t_r. In real situations, the air-vapor power plant may be an open-cycle system and at this point, the exhaust air-vapor mixture out of the regenerator is discharged into the ambient. However, like many other thermodynamic cycle analyses, it could be modeled as a closed-cycle system herein. Therefore, a constant pressure process with further vapor mass and heat removal is added, and the moist air returns to its starting point of the cycle to complete the cycle. During this process, an amount of vapor mass, $W_r - W_o$, as marked in the *t-s* diagram in Fig. 5a, left the moist air and enters the ambient air. It should be pointed out that possible water recovery between W_r and W_o could be added, as shown in Fig. 4, so that most of the vapor water left the regenerator could be collected without being lost to the ambient.

Figure 5b shows a thermodynamic cycle of the water associated with the operation of the power plant in terms of a t_w vs. r_{wa} diagram with certain idealizations, wherein r_{wa} is the ratio of water flow rate $\dot{m}_w$ to the dry air mass flow rate $\dot{m}_a$. The hot water from a hot-water storage facility or a heat source enters a direct-contact heat-mass transfer packing with a temperature t_{w1} and a mass flow rate of r_{wa1}. After the mass and heat transfer from the hot water into the air-vapor mixture in the packing, the water leaves the packing with reduced temperature and mass flow rate, respectively at t_{w2} and r_{wa2}. The mass removal from the water in the packing, $r_{wa1} - r_{wa2,}$ is marked in the packing process in Fig. 5b. Then the colder water enters a regenerator condenser, wherein the vapor in the hotter air-vapor mixture condenses, releasing its condensation heat. The water receives the released condensation heat and raises its temperature to t_{wr}, which may be close to t_e in Fig. 5a. At the same time, water receives the condensate mass associated with the vapor condensation and increases its mass flow rate to r_{war}. Therefore, at the outlet of the regenerator, the water has an increased temperature, and through makeup water addition, the water would regain its original mass of r_{wa1}, or $r_{war} = r_{wa1}$. Obviously, this is an assumption for a better description of the cycle. The mass addition to the water in the regenerator, $r_{wa1} - r_{wa2}$, is also marked in Fig. 5b. The water leaving the regenerator is then thermally recharged by a heat source and its temperature is raised back to $t_{wa1}$to return to the packing and complete the cycle

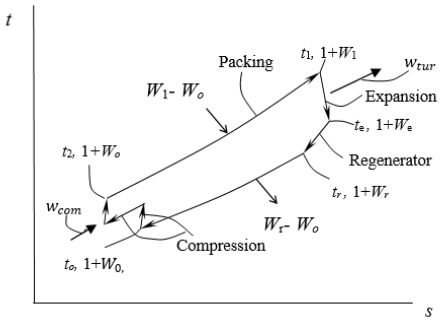

(a)

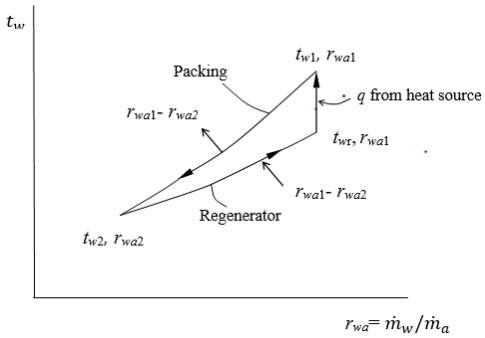

(b)

Fig. 5: Thermodynamic cycles associated with Figs. 1 and 4: (a) Air-vapor mixture in terms of a *t-s* diagram and (b) The water in terms of temperature t_w vs. water mass per kg dry air r_{wa}.

4. PERFORMANCE EVALUATION MODEL AND RESULTS FOR POWER PLANT CONFIGURATION IN FIG. 1

As discussed earlier in this paper, a major difference between the present air-water power plant and the conventional gas turbine power plant is the heat acquisition of the working fluid before the expansion in the turbine. In a conventional gas turbine power plant, the heat acquisition is through fossil fuel combustion in a combustion chamber. In the present air-water power plant, however, the heat acquisition is through mass and heat transfer from the hot water to the moist air working fluid in a packing. Although with different operational objectives, the working mechanism of the packing may be similar to that of a cooling tower. In a cooling tower application, the objective is to cool a water flow from a given inlet temperature to the desired outlet

temperature, so the inlet and outlet water temperatures are normally specified in the performance calculation. The moist air condition at the outlet of the packing is still needed in the calculation procedure (Moran et al., 2011; Hewitt et al., 1994), but it is not a performance objective of the system. The water flow rate per kg of dry air is also an important parameter, and it can be calculated through an overall energy balance over the packing if the moist air condition at the outlet is known.

In the present air-water power plant calculations, the condition of the air-vapor mixture at the outlet of the packing is a performance objective. Therefore, in this calculation model, the air-vapor mixture condition at the outlet of the packing is specified along with the specified hot water inlet temperature to the packing and water outlet temperature out of the packing, while the hot water mass flow rates into and out of the packing are calculated through the overall energy and mass balances on the entire packing. The condition of the air-vapor mixture at the packing outlet can be specified in terms of the mixture temperature and the humidity ratio. According to the cooling-tower experimental data of Zengin and Onat (2020) and Leeper (1981), the moist air at the outlet of the packing is normally saturated even at a rather low air temperature of 35ºC for cooling tower applications. In the present application, the hot water temperature is much higher, around the level of 100ºC. Because the vapor pressure increases exponentially with temperature and the vapor mass flux intensity at the water-air interface in the packing is at least one order of magnitude higher than that at 35ºC, the saturation condition of the air-vapor mixture should be satisfied. Therefore, based on Eq. (3), the humidity ratio of the air-vapor mixture at the outlet of the packing is calculated by the following relation:

$$W_1 = W_{1s} = 0.622\frac{p_s(t_1)}{(p_t - p_s(t_1)}} \tag{4}$$

The temperature of the air-vapor mixture at the outlet of the packing should reasonably approach the hot water inlet temperature because of the counterflow arrangement, two-phase direct-contact heat mass transfer, and large transfer surface area created by the packing. However, reaching the exact hot water temperature may demand an unreasonable height of the packing. Therefore, the temperature of the air-vapor mixture at the outlet of the packing is specified based on a packing efficiency defined by the following relation:

$$\eta_{packing} = \frac{t_1 - t_2}{t_{w1} - t_2} \tag{5}$$

where t_1 is the temperature of the air-vapor mixture exiting the packing, t_2 is the moist air temperature entering the packing, which can be found through the compressor-related calculation with given ambient air condition, and t_{w1} is the hot water temperature entering the packing ($t_{w1} = t_w$ without considering the flashing effect at the packing top). In a single-phase, gas-to-gas heat exchanger, a heat exchanger efficiency of 80% is possible. Because of the two-phase, direct-contact heat mass transfer, and large transfer surface area, a packing efficiency of 95% is used to calculate t_1.

The packing-related calculation would also involve dry air enthalpies at the packing inlet and outlet, h_{a2} and h_{a1} and the vapor enthalpies at the packing inlet and outlet, h_{v2} and h_{v1}. But they can be calculated with the respective temperatures under ideal gas conditions. Similarly, the enthalpies of water at the packing inlet and outlet, h_{w1} and h_{w2} can be calculated by using their respective temperatures. Energy and water mass balances over the packing would respectively produce the following two equations:

$$r_{wa1}h_{w1}(t_{w1}) + (h_{a2}(t_2) + W_o h_{v2}(t_2)) - r_{wa2}h_{w2}(t_{w2}) - (h_{a1}(t_1) - W_1 h_{v1}(t_1)) = 0 \tag{6}$$

$$r_{wa2} = r_{wa1} - (W_1 - W_o) \tag{7}$$

By knowing $t_{w1}, t_{w2}, t_1, t_2, W_1, W_o$, the hot water mass flow rate r_{wa1} at packing inlet, and the colder water mass flow rate exiting the packing r_{wa2} can be found from the above two equations.

In the cooling tower for air conditioning applications, one of the most important specifications is "approach" which is defined as the difference between the temperature of the cold water leaving the cooling tower and the wet-bulb temperature of entering air. In some performance specifications, the "approach" is less than 5ºC (McQuiston et al., 2005). When the ambient air entering the tower has a relatively low relative humidity, the wet-bulb temperature may be more than 10ºC lower than the dry-bulb temperature of the ambient air. In other words, the water could be cooled more than 5ºC below the ambient temperature. This could be the case for the present power plant application because of the much higher working temperature accompanied by a much higher interface vapor flux, which is beneficial for a higher thermal efficiency in conjunction with the use of a regenerator. However, because the primary purpose of this paper is to introduce the concept of the air-water power plant, the calculation would take a simplified, yet conservative, approach by limiting the packing outlet water temperature to close to the inlet moist air temperature, or $t_{w2} \approx t_2$.

Like many other thermal power plants, two of the most important outcomes to gauge the performance of the power plant in this paper are network output w_{net} and thermal efficiency η_{th}in a cycle, which are respectively shown below:

$$w_{net} = w_{tur} - w_{com} \tag{8}$$

$$\eta_{th} = \frac{w_{net}}{q_{HS}} = \frac{w_{net}}{r_{wa1}(h_w - h_{wr})} \tag{9}$$

where w_{tur} is the turbine work output per kg dry-air, w_{com} is the compressor work input per kg-dry air, q_{HS} is the heat input from the heat source to the power plant per kg-dry air, h_w is the hot water enthalpy entering the power plant ($h_w = h_{w1}$ without flashing effect), and h_{wr} is the water enthalpy leaving the power plant. Because of the use of the regenerator condenser, the water enthalpy at the outlet of the regenerator is used in the calculation. By knowing the network per unit mass of dry air, the power capacity of the power plant can be calculated by the following:

$$P = \dot{m} \times w_{net} \tag{10}$$

where $\dot{m}$ is the mass flow rate of dry air, which can be found through the power plant size *D* measured at the inlet of the compressor system in Fig. 1 and the average air velocity *V* associated with the size *D*. Like conventional gas turbine power plants, the most serious irreversible losses in the present power plant are related to the irreversibility in the compressor and turbine systems. In this model calculations, the related irreversibility is taken into account through the specifications of isentropic compressor-system efficiency η_c and isentropic turbine efficiency η_t, which are taken to be 90% and 95%, respectively. Also, the calculation is based on conditions that two intercoolers are employed with the moist air being cooled back to the ambient temperature after the intercooler. In the regenerator, the cold water entering the regenerator is assumed to be heated to the inlet temperature of the air-vapor mixture because of the high regenerator efficiency associated with direct-contact condensation and the use of the packed bed. Finally, the pressure drops across the packing or bed are not included, since the pressure drop across the packing is generally less than 100 Pa, two orders of magnitude lower than the pressure of the air-vapor mixtures after the compressor system. To avoid the use of constant properties in the calculations, properties data are correlated by polynomials and maximum errors between those calculated through the polynomial relations and the data from the properties tables are generally about 1%. In this simplified modeling, only some definitions and computational procedures unique to the air-water power plant are

presented. More comprehensive modeling would involve packing design, which could be a future publication but is not the subject of this paper for the general performance trend of the air-water power plant.

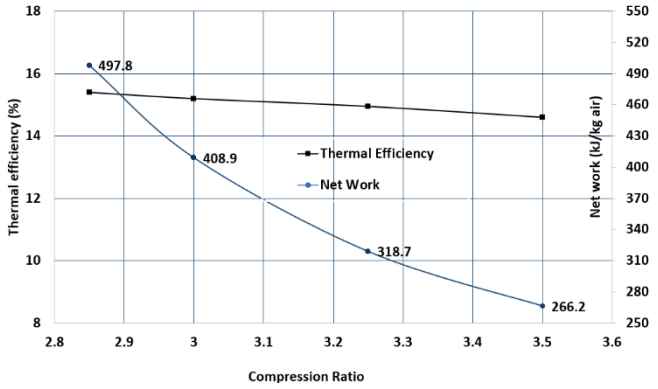

Fig. 6a: $t_{w1} = 130^o C$

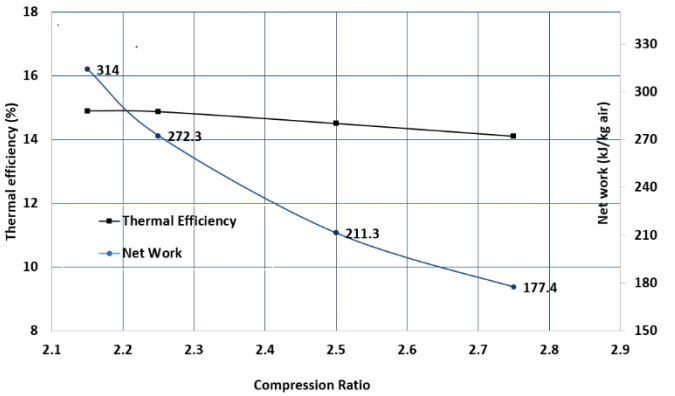

Fig. 6b: $t_{w1} = 120^o C$

Figures 6a to 6d present some model calculation results for power plant thermal efficiency and network output as a function of compression ratio at different hot-water inlet temperatures as the heat source. At a given hot water inlet temperature, the thermal efficiency is not very sensitive to the compression ratio because of the use of a regenerator; but the network drops very significantly as the compression ratio (or operating pressure) is increased, which can be explained through Eq. (4). For a given operating temperature or a partial vapor pressure, an increased total pressure (operating pressure) through an increase in compression ratio will decrease the humidity ratio or the vapor amount per kg dry air into the turbine, which would reduce the turbine power output accordingly. On the other hand, for the same total pressure, a higher hot-water temperature would link to a higher vapor partial pressure, which would increase the humidity ratio or the vapor mass entering the turbine. Because the saturated partial vapor pressure increases exponentially with an increase in temperature, the network output would accordingly increase very significantly with an increase in hot-water inlet temperature, as shown in the above figures.

The network outputs as presented in the above figures are in terms of work output per unit air flow rate. The total power-plant capacity can be calculated by knowing the power plant size, which is designated by the diameter D shown in Fig. 1 at the inlet of the compressor system, and the air velocity at that location. If the diameter D = 6 m, and the corresponding average air velocity is V = 10 m/s, the airflow rate would be:

$$\dot{m} = \rho \frac{\pi}{4} D^2 V = 1.22 \times \frac{\pi}{4} 6^2 \times 10 = 345.0 \text{ kg dry air/s} \qquad (11)$$

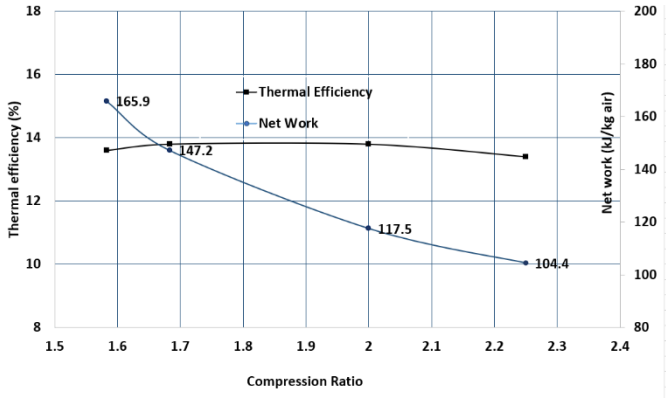

Fig. 6c: $t_{w1} = 110^o C$

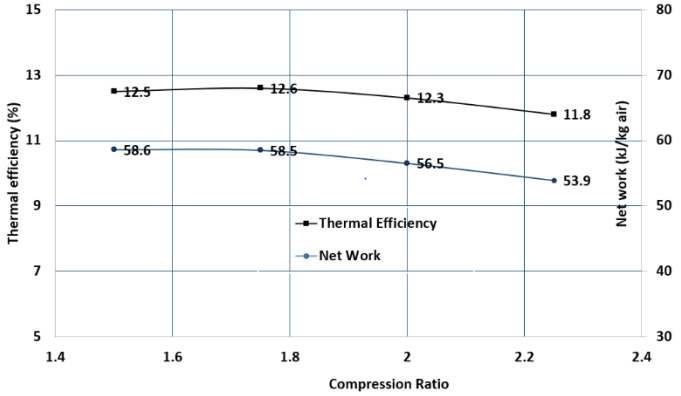

Fig. 6d: $t_{w1} = 100^o C$

Fig. 6: Power plant thermal efficiency (left) and network output per unit dry-air (right) as a function of compression ratio at different hot water inlet temperatures (Figs. 6a-6d).

Then, the power capacity can be calculated by using Eq. (10). The use of a large diameter D was justified because of the operating conditions of low temperature and pressure.

Table 2 summarizes some typical results along with the power capacity and the second law efficiency at several hot water inlet temperatures t_{w1}. As can be seen, at a low-mid temperature of 130°C, the power capacity has reached more than 170 MW, matching the capacity of large fossil-fuel-burning power plants. The thermal efficiency is also fairly good, above 15%. At a lower end of the hot water temperature, such as t_{w1} = 100°C, the thermal efficiency still maintains a fairly good value of above 12.5%, but the power capacity is reduced to about 20 MW.

Table 2: Performance results for the power plant shown in Fig. 1 at t_o = 15°C.

t_{w1} (°C)	Compression ratio	w_{net} (kJ/kg dry air)	Power capacity (MW)	Thermal efficiency (%)	Second-law efficiency (%)
130	2.85	497.8	171.7	15.37	53.9
120	2.25	272.3	93.9	14.9	55.8
110	1.583	165.9	57.2	13.6	54.8
100	1.5	58.6	20.2	12.51	54.9
90	1.75	30.84	10.6	10.9	52.66

In the above calculation results, the ambient air is set at 15°C which is a standard temperature for thermal power plant evaluations in the industry. This temperature may be reasonable for the winter or year-round average; but in the summer, the average ambient temperature should be much higher than that. The power plant performance may be significantly affected by a higher ambient temperature even for some conventional steam-turbine-based fossil-fuel power plants. However, the impact of the higher ambient temperature will be much more severe for the present air-water power plants under low operating temperatures. To alleviate this problem, a technique to use a chiller to cool the intake air of the power plant, the inlet air of a compressor system, or the intercooler air may be employed. Figure 7 shows schematically the cooling of an intercooler air by a chiller. To quantitatively demonstrate the effectiveness of this technique, the results in Table 2 are used as a base for comparison. In this case, a centrifugal chiller was used to cool the second intercooler air after the ambient temperature and relative humidity were increased, respectively, to t_0 = 35°C and W_o = 0.018 vapor/dry air, which may represent weather conditions for summer. Like other refrigeration systems, the chiller's performance is gauged by its coefficient of performance (COP) as defined by the following relation.

$$COP = \frac{Heat\ removal}{work\ input} \tag{12}$$

To reduce the power consumption of the chiller, the intercooler as shown in Fig. 7 was divided into two sections. The lower section is cooled by the water from a cooling tower of the chiller to reduce the air temperature to near the ambient temperature of 35°C before the air is directed to the upper section of the intercooler for chiller cooling. It should be mentioned that the cooling tower in Fig. 7 may be replaced by a dry-cooling system for water conservation. For comparison purposes, in the second section of the intercooler, the chiller would cool the air to the condition of t_0 = 15°C and W_o = 0.005 vapor/dry air, which is the ambient condition used for the results in Table 2, before the air is directed to the next compressor.

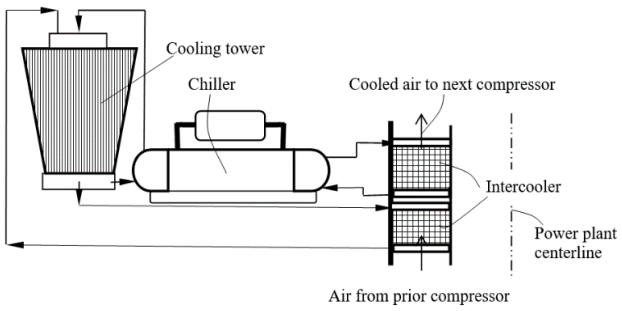

Fig. 7: A schematic illustration of a chiller system to cool the intercooler air of a compressor system.

For the case of t_{w1} = 120°C and a compression ratio of 2.25 under the ambient air condition of t_0 = 35°C and W_o = 0.018 vapor/dry air with the incorporation of the chiller cooling on the second intercooler, computer program calculation was undertaken and the results for the network output and thermal efficiency are respectively given below:

w_{net} = 263.4 kJ/kg-dry air, η_{th} = 14.11%.

However, the results above must be corrected due to the work consumption of the chiller to achieve the cooling effect. The centrifugal chiller generally has a much higher COP than a residential air conditioning system, and a COP of 8 to 9 is not uncommon (HVAC HESS, 2022; Evans, 2017; and Daikin, 2020). The chiller work consumption can be calculated by the following relation on the basis per kg of dry air by using a chiller COP of 8:

$$w_{chiller} = \frac{\Delta h}{COP} = \frac{20.27}{8} = 2.53 \frac{kJ}{kg\ dry\ air}$$

where Δh is the enthalpy drop between the condition of t_0 = 35°C, W_o = 0.018 and the condition of t_0 = 15°C, W_o = 0.005. Then, the corrected network and thermal efficiency are respectively shown below:

$$w_{net,c} = 263.4 - 2.53 = 260.87 \frac{kJ}{kg\ dry\ air}$$

$$\eta_{th,c} = 14.11 \times \frac{260.87}{263.4} = 13.97$$

Compared to the result shown in Table 2 with the ambient condition of T_0 = 15°C, W_o = 0.005 without chiller cooling, the new work output, and thermal efficiency decreased, respectively, by about 4.5% and 6%. For the case of t_{w1} = 100°C and a compression ratio of 1.5 under the air inlet condition of t_0 = 35°C, W_o = 0.018, calculations were also done under similar chiller cooling procedures, and results are summarized in Table 3 along with the results of t_{w1} = 120°C.

Table 3: Results for ambient conditions of t_0 = 35°C, W_o = 0.018, with intercooler cooling by a chiller, as compared to the results of t_0 = 15°C, W_o = 0.005 from Table 2.

t_{w1} (°C) (t_o = 35°C)	Compression ratio	Network (kJ/kg dry air) (Change over the case of t_o = 15°C)	Thermal efficiency (%) (Change over the case of t_o = 15°C)
120	2.25	260.87 (-4.5%)	13.97 (-6%)
100	1.5	52.51 (-10.3%)	10.3 (-11.2%)

The results in Table 3 show that when the chiller cooling technique is employed, the negative impact of a higher ambient temperature is not significant except for a lower operating temperature.

5. THE EMBODIMENT WITH VACUUM-PUMP COMPRESSOR

According to the performance results in Table 2 associated with the power plant embodiment in Fig. 1, when t_{w1} is equal to or below 100°C, power output dropped sharply accompanied by a significant reduction in thermal efficiency. Also, the air-vapor mixture is unable to expand through the turbine to backpressure lower than the ambient pressure, as is the case for most conventional steam-turbine power plants. The low power output is believed due to the mismatch between the operating temperature and operating pressure, with a higher operating pressure but at a lower operating temperature. As discussed, the turbine power production is determined by the inlet enthalpy of the working fluid according to Eq. (1), which in turn is largely determined by the humidity ratio W for the present operation. According to Eq. (4) for W, at a given maximum operating temperature, a higher total or operating pressure would diminish the humidity ratio. A reduced operating pressure through the reduction of compression ratio would increase the humidity ratio but would reduce the turbine expansion ratio, which would also hurt the turbine work output.

Figure 8 shows schematically another embodiment of the air-water power plant unit (Cao, 2022b), which would significantly improve the performance for the hot water temperature equal to or below 100°C. In this case, a vacuum pump or compressor system is employed after the regenerator condenser to create a turbine outlet pressure lower than the ambient pressure and also to discharge the exhaust air out of the power plant unit. For the hot water temperature equal to or below 100°C, the turbine inlet pressure may be close to the ambient pressure for a higher humidity ratio with still sufficiently high turbine expansion ratio because of the lowered turbine backpressure.

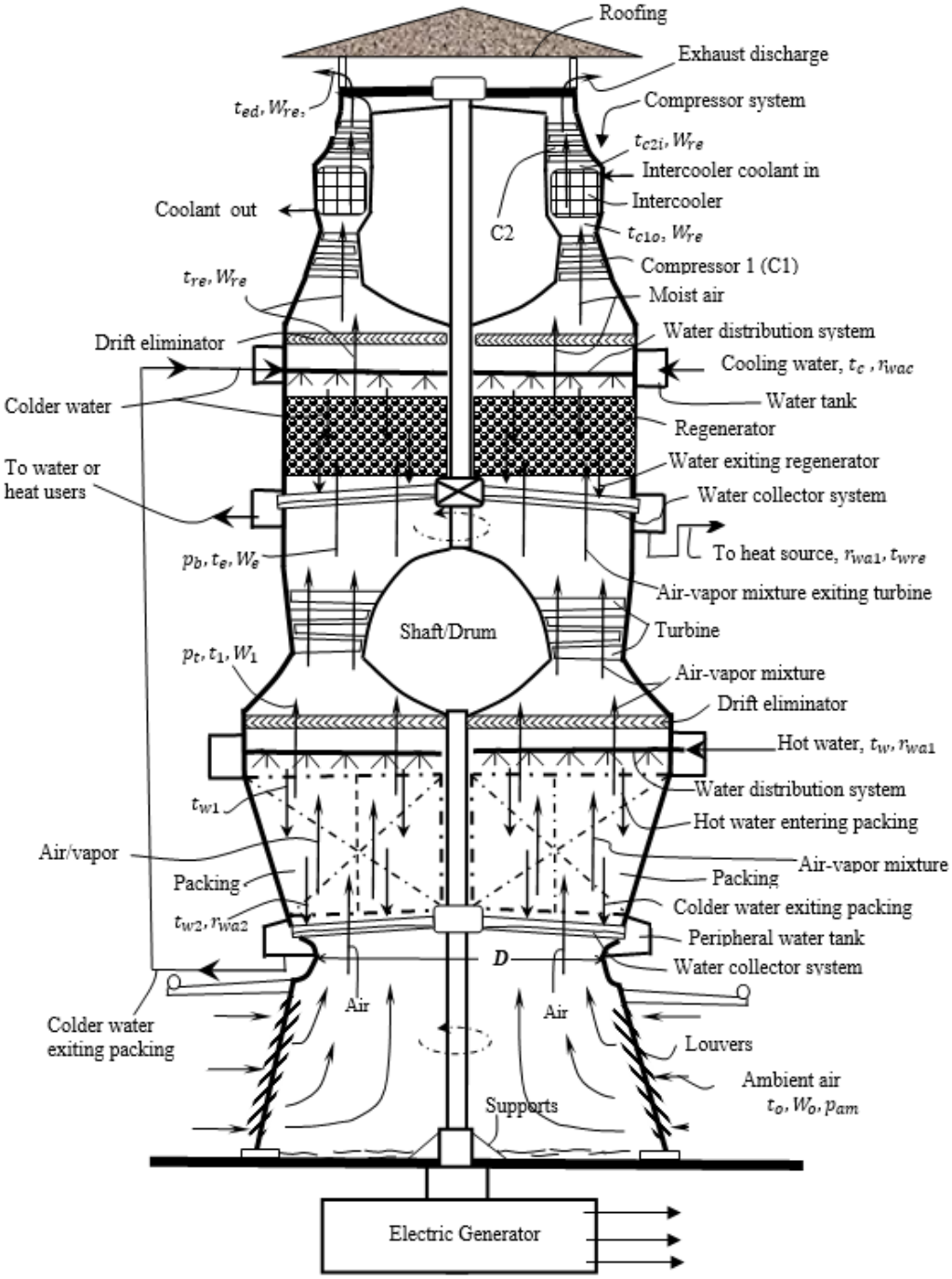

Fig. 8: A schematic vertical sectional view of an air-water power plant employing a vacuum-pump compressor system to maintain turbine backpressure below the ambient pressure and discharge the exhaust air.

Referring to Fig. 8 and starting from the bottom of the power plant, ambient moist air at t_o and W_o is induced into the power plant through an air inlet section with louvers. A fan may be deployed for air intake purposes, but this may not be necessary in many cases. The air converges and flows upward into a packing from the bottom to acquire latent and sensible heat from the counterflowing hot water flow stream. Similar to the packing in Fig.1, it has an associated hot water distribution system, a colder water collector system, and a peripheral

Global Digital Central
ISSN: 2151-8629

water tank. The packing, hot water distribution system, the colder water collector system, and peripheral water tank have been described associated with Fig. 1 and will not be repeated herein. Hot water, as the energy-supply fluid of the power plant with a temperature t_w and mass flow rate of r_{wa1}, based on the unit mass of the dry air, enters the power plant through the water distribution system. The hot water leaves the distribution system and enters the packing from the top at a temperature of t_{w1}. If the hot water flashing through the distribution system is neglected, $t_{w1} = t_w$, with the same water flow rate. Through the intimate heat and mass transfer in the packing from the hot water to the airflow stream, the moist airflow may essentially become an air-vapor mixture, due to the significantly increased vapor content.

After the energy acquisition in the packing, the air-vapor mixture exits the packing with an increased humidity ratio W_1 and an increased temperature t_1, but its pressure p_t may be close to the ambient pressure p_{am} as the pressure drop through the packing may be generally small, as shown on the left side of Fig. 8. Upon passing through a drift eliminator to remove liquid droplets, the air-vapor mixture is ducted into a turbine to produce power through expansion from p_t to turbine backpressure that may be significantly lower than the ambient pressure. After the expansion and converting some of the thermal energy content into power, the air-vapor mixture exits the turbine with reduced pressure p_b, temperature t_e, and humidity ratio W_e, wherein p_b is the turbine outlet pressure or backpressure, as shown in Fig. 8. However, the air-vapor mixture exiting the turbine still contains a large amount of unused thermal energy, particularly in terms of vapor content in the mixture. Therefore, a regenerator condenser is employed to recover a significant amount of the energy and water from the mixture, and the air-vapor mixture would continue its flow path to enter the regenerator. Similar to the case in Fig. 1, the regenerator in Fig. 8 may be a counter-flow, direct-contact condenser with a packed bed.

The colder water with a reduced temperature of t_{w2} and a lower water mass flow rate of r_{wa2}, exits the packing before the turbine and is collected by the water collection system of the packing, which is then pumped from the water tank of the packing to a water distribution system of the regenerator on top of the regenerator through a peripheral water tank of the regenerator. Meanwhile, the air-water mixture enters the regenerator condenser from the bottom of the regenerator with t_e, W_e, and leaves the regenerator as moist air with a significantly reduced temperature t_{re} and vapor content W_{re}. After passing through a drift eliminator, the moist air out of the regenerator enters a vacuum pump or compressor system.

The pressure in the regenerator should be close to the turbine backpressure as the pressure drop through the regenerator is generally small. The backpressure, p_b, should be sufficiently lower than the ambient pressure to create a sufficient expansion ratio for the operation of the turbine. In this case, a vacuum-pump compressor system is employed to maintain the lower pressure at the outlet of the turbine while raising the pressure of the moist air out of the regenerator to discharge it into the ambient. The vacuum pump compressor system as shown in Fig. 8 is an axial compressor system, but it could be a centrifugal compressor system or other vacuum pump systems. To reduce the power consumption of the compressor system, at least an intercooler may be employed.

Referring to the compressor system in FIG. 8, the moist air at t_{re} and W_{re} enters the first compressor (C1) and is compressed to t_{c1o}. The moist air then enters an intercooler, and its temperature is cooled down to t_{c2i}. Finally, the moist air enters a second compressor (C2) and is compressed to near ambient pressure to be discharged into the surroundings. To prevent the power plant from being flooded under rainy or snowing conditions, a roofing structure may be installed on top of the power plant.

It is well known that the power consumption of a compressor system is not only sensitive to the inlet temperature of the air but also sensitive to the moisture in the air. In this consideration, the mass flow rate of colder water out of the packing and being pumped into the regenerator condenser may not be enough to reduce the temperature and vapor content of the moist air out of the regenerator to a satisfactorily low level. Therefore, an additional cooling water flow stream with a temperature of t_c and a mass flow rate of r_{wac} maybe added to the regenerator condenser, with t_c preferably being close to the ambient temperature, as shown on the right side of the regenerator. Because of the cooling water addition, the water with increased temperature and mass exiting the regenerator condenser at the bottom may have two destinations. The first destination, similar to the case of Fig. 1, is a thermal storage system or a heat source to be thermally recharged, as shown on the right side of the water collector system of the regenerator, and the thermally recharged water may return to the power plant as heat-supply hot water into the packing, as shown on the right side of the water distribution system of the packing. The second destination could be heat or water users as shown on the left side of the water collector system of the regenerator. In addition to reducing the temperature and vapor content of the moist air at the inlet of the compressor system for power consumption reduction, the addition of the cooling water would enable the power plant to supply hot water for various users or into storage for future uses. In Fig. 8, the two water outflow streams from the regenerator are extracted at the bottom of the regenerator, but the extraction could be at any suitable location of the regenerator. Also, the regenerator as shown in Fig. 8 is essentially the combination of a regenerator and a heat or water recovery unit.

To enhance the understanding of the system shown in Fig. 8, a flow diagram demonstrating the operation principle of the power plant is shown in Fig. 9a, wherein q_{IC} is the heat removal from the intercooler of the vacuum-pump compressor system. The pressure distribution of the working fluid along with the height Z of the power plant is also schematically shown in Fig. 9b. The ambient air enters the packing at an ambient pressure p_{am} (point 1). Air-vapor mixture exits the packing with a slight pressure drop (point 2), and then enters the turbine to produce power. The air-vapor mixture exits the turbine (point 4) with a turbine backpressure p_b. Then it enters a regenerator/heat-water recovery unit at point 5. With significantly reduced vapor content and temperature, the air/vapor or moist air exits the regenerator at point 6 and enters the vacuum-pump compressor system at point 7. Finally, at point 8, the moist air is compressed to the ambient pressure p_{am} for discharging into the ambient.

Performance evaluation was undertaken for the power plant with a vacuum-pump compressor system as shown in Figs. 8 and 9 at different hot water inlet temperatures t_{w1} and turbine outlet pressure or backpressure p_b. For all the results from the evaluation, the ambient temperature was set at t_{am} = 15ºC, the isentropic efficiencies for compressor and turbine systems were, respectively, set at 90% and 95%, the packing efficiency was 0.96, and the power plant diameter was also set as D = 6 m with the same air velocity of 10 m/s, which gave the same dry air mass flow rate from Eq. (11).

The temperature of the cooling water t_c in Figs. 8 and 9 was 20ºC, five degrees higher than the ambient temperature, and the temperature of the moist air out of the regenerator and entering the vacuum-pump compressor system t_{re} was 22ºC, two degrees higher than the cooling water inlet temperature. One intercooler was deployed between the first and second compressors of the compressor system. The temperatures of the two water-flow streams out of the regenerator, respectively, to the storage/heat source and to the heat/water users, were set at two degrees lower than the temperature t_e of the air-vapor mixture into the regenerator. The basic evaluation model in Section 4 of this paper was used for the work of this section, and its description is not repeated herein.

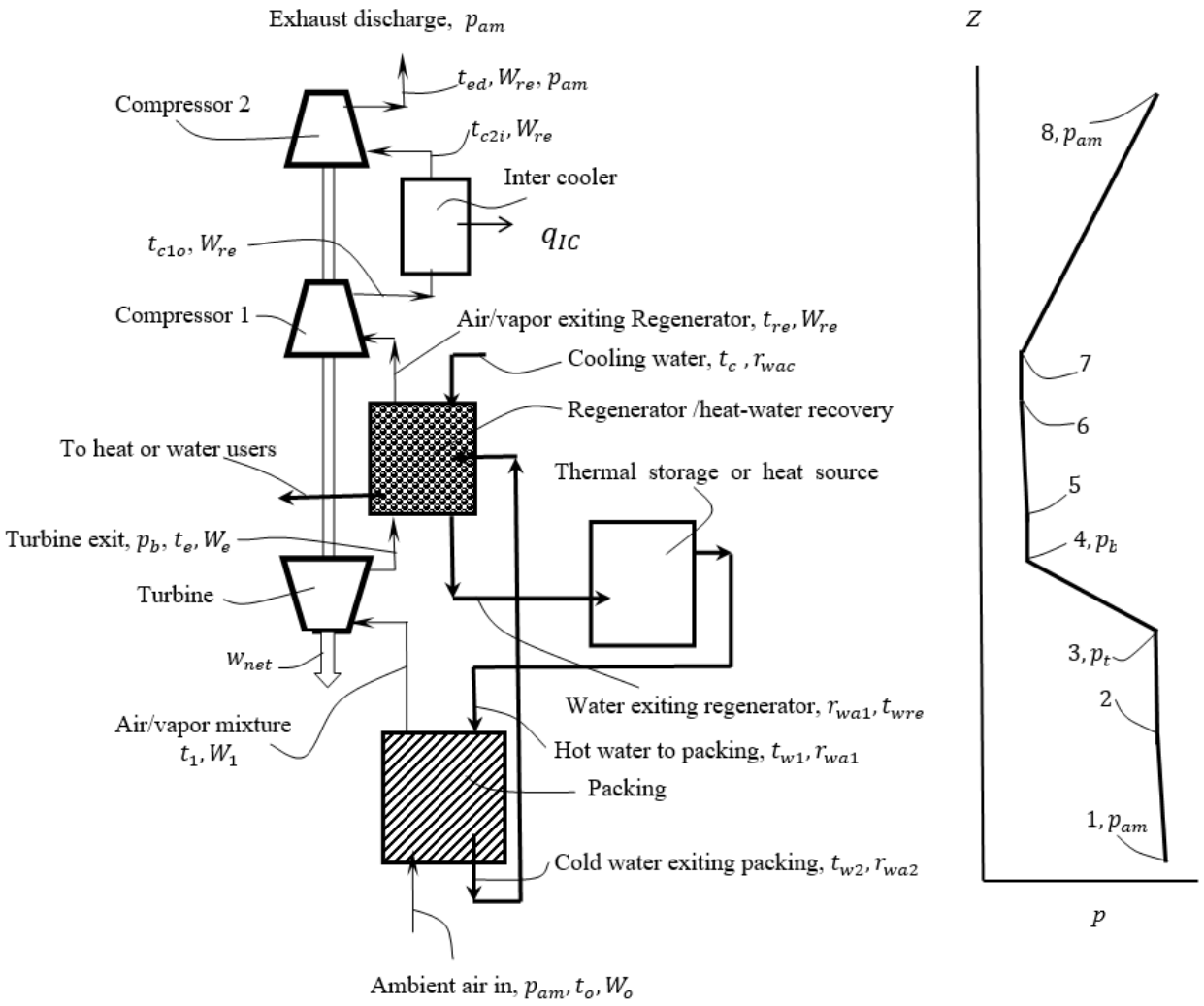

Fig. 9: A flow diagram demonstrating the operation principle of the power plant as shown in Fig. 8 (Fig. 9a) and a schematic working-fluid pressure distribution along with the height of the power plant (Fig. 9b).

Figure 10 shows thermal efficiency (left) and network output per unit mass of dry air (right) as a function of the turbine outlet pressure at a hot water inlet temperature to the packing of 100ºC. As can be seen, at a turbine outlet pressure of 0.25 bar, the net power output had reached more than 885 kJ/kg dry air while the thermal efficiency was above 15%. The very significant improvement over the first embodiment was due to the good match between the operating pressure and temperature, resulting in a high humidity ratio of about 4.91 (please see more detailed information in Table 1 for the case of 96.6ºC that is the air-vapor temperature before the expansion in the turbine), which would significantly increase the power output of the turbine. This case also benefited from a higher turbine expansion ratio from almost ambient pressure to an outlet pressure of 0.25 bar.

For some hot water temperatures lower than 100ºC under low turbine backpressure, the power consumption of the vacuum-pump compressor system was too high relative to the power output of the turbine due to excessive vapor content entering the compressor system. For this reason, a centrifugal chiller, similar to the frontal compressor system in Fig. 1, was used to cool the air/vapor mixture or moist air out of the regenerator to 10ºC below the ambient temperature before entering the compressor system to significantly remove the vapor content in the moist air. Then the net power output and thermal efficiency of the power plant were corrected based on the power consumption of the chiller.

Figure 11 presents performance results at different hot water temperatures with chiller cooling. Comparing the two cases in Fig. 10 and Fig. 11a with the same hot water temperature of 100ºC, the performance improvement with the chiller cooling over that without the chiller cooling is meaningful. It should be noticed that although by general standard the performances were very impressive for cases of Figs. 11b-11d with hot water temperatures below 100ºC, the power capacity drops sharply as the hot water temperature is reduced below 100ºC. This was caused by the mismatch between the operating temperature and pressure. Within a temperature range near 100ºC, a slight temperature decrease would cause a significant vapor pressure decrease, but in these cases the operating pressure remains almost the same near the ambient pressure. The combination of these two factors would result in a much lower humidity ratio, which would decrease the turbine power output.

Some typical results including the power capacity and second law efficiency of the power plant with or without chiller cooling are summarized in Table 4. The power capacity of the air-water power plant employing a back vacuum-pump compressor system improved dramatically at low hot-water temperatures equal to or below 100ºC. The best result in the Table shows that the power capacity and second-law efficiency have reached more than 330 MW and 70%, respectively, matching the performance of some fossil-fuels-based power plants. The power capacity could be further increased by increasing the diameter D, as the maximum pressure difference across the plant is less than 1 bar.

Although the results in Table 4 are for a lower ambient temperature of 15ºC, the power plant could also work at a much higher ambient temperature with limited penalties. This can be accomplished by using a chiller to cool the intake ambient air or the flow streams through any part of the compressor system including the intercooler. Since the chiller cooling effects have been demonstrated earlier in this paper associated with the embodiment in Figs. 1 and 2, the demonstration for the embodiment related to Figs. 8 and 9 is not repeated.

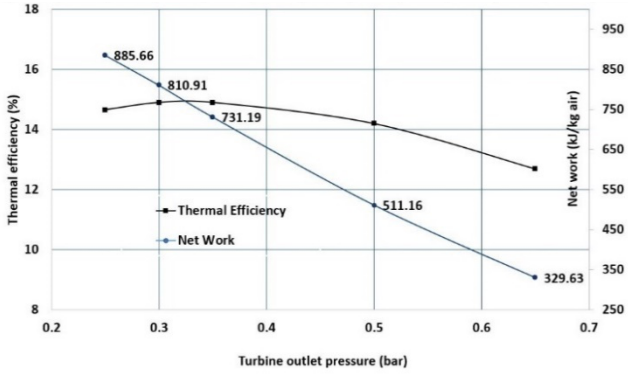

Fig. 10: Thermal efficiency (left) and new work output per unit dry-air (right) as a function of the turbine outlet pressure at a hot-water inlet temperature to the packing of 100ºC.

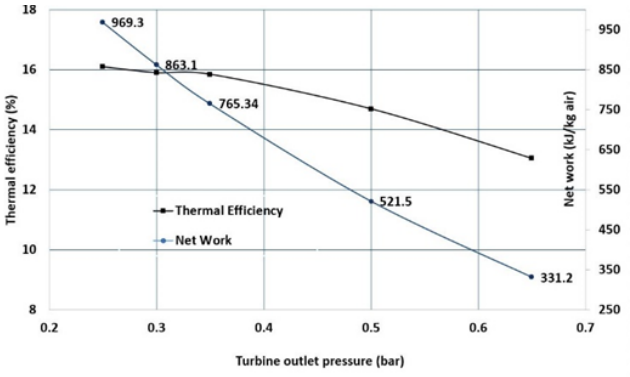

Fig. 11a: t_{w1} = 100ºC

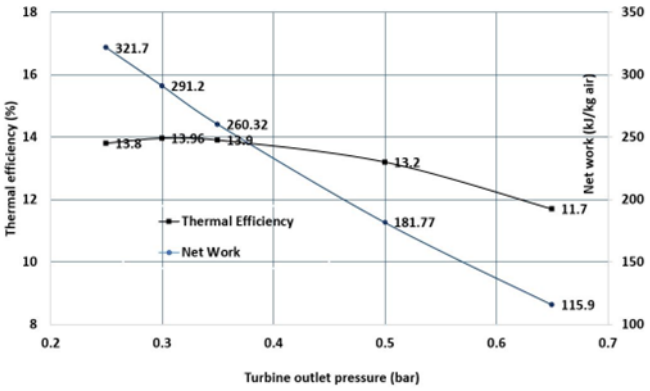

Fig. 11b: t_{w1} = 95ºC

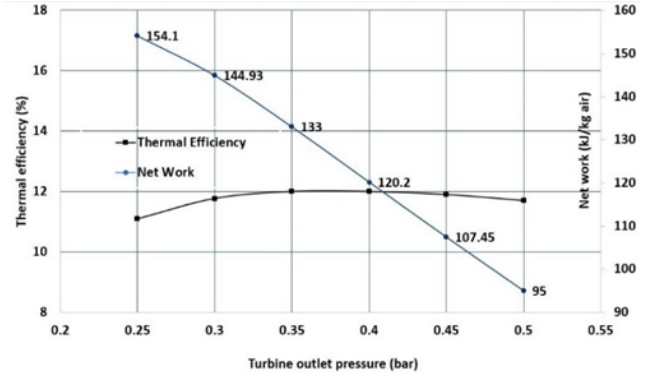

Fig. 11c: t_{w1} = 90ºC

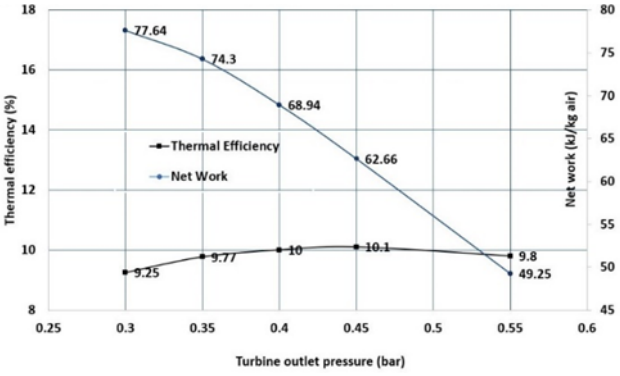

Fig. 11d: t_{w1} = 85ºC

Fig. 11: Performance results at different hot-water inlet temperatures as a function of turbine outlet pressure with chiller cooling.

Table 4: Summary of some typical results for power plants with vacuum-pump compressors.

t_{w1} (°C)	Turbine back pressure (bar)	Chiller cooling?	w_{net} (kJ/kg dry air)	Power capacity (MW)	Thermal efficiency (%)	Second-law efficiency (%)
100	0.25	no	885.7	305.6	14.66	64.3
100	0.25	yes	969.3	334.4	16.1	70.6
95	0.25	yes	321.7	111.0	13.8	63.6
90	0.30	yes	144.9	50.0	11.8	57.0
85	0.4	yes	68.9	23.8	10.0	51.0

In the performance evaluations of this paper, hot-water flash at the exit of the water distribution system of the packing was not considered; therefore, $t_{w1} = t_w$, indicating that the hot water inlet temperature to the packing is the same as the hot water inlet temperature to the power plant. In reality, hot-water flash may occur, and the hot-water temperature at the inlet of the power plant would be higher than that at the inlet of the packing. For the embodiment in Fig. 8, the water flash would be an important operational mechanism for a hot water temperature higher than 100°C at the inlet of the plant. In this case, the vapor generated by the water flashing would join the air-vapor mixture out of the packing into the turbine, while the remaining water after the flashing would enter the packing. The outcome would be improved performance of the power plant, primarily due to the increased vapor mass entering the turbine. For the embodiment shown in Fig. 1, if the hot-water temperature and pressure entering the plant are high and a higher pressure of the air-vapor mixture to accommodate the high hot water temperature/pressure is not desirable, the compressed hot water could flash into lower pressure water before entering the packing. In addition to flashing through the hot-water distribution system, a separate flash chamber may be employed, which would substantially separate the generated vapor to the turbine and the remaining water to the packing. The first embodiment in Fig. 1 is essentially a frontal compression system while the second embodiment is a rear compression system, each of which would have its own merits under different conditions. However, both frontal and rear compression systems may be combined for a power plant, although with somewhat increased complexity. Also, the reheat mechanism that is sometimes used for conventional gas turbine power plants may be adopted for the present air-water power plant. The above-mentioned mechanisms or deployments are not described in detail in this paper but have been addressed by Cao (2022b) among other considerations.

6. DISCUSSIONS AND CONCLUSIONS

1. This paper introduced the concept of the air-water thermal power plant and its embodiments for utility-scale power production and heat supply at low temperatures. Performance evaluations indicated that at a heat source temperature near 100°C, the new power plant could achieve a power capacity of more than 300 MW and a thermal efficiency of above 15%. Combined with hot-water storage systems, the power plant could enable the use of the most available renewable energy sources such as solar and geothermal energies as well as industrial waste heat to generate dispatchable power reliably. In addition, the power plant uses natural and clean substances as the working fluids and thermal-energy storage media with minimized environmental impacts. Thus, the new renewable-energy-based power plants could replace the role of fossil-fuel-based power plants to serve as a backbone or baseload of national power grids.
2. It is well known that a conventional gas-turbine power plant must work at a very high temperature. As a result, expensive metals such as nickel-alloy-based exotic high-temperature materials may be used for critical components, and the costs of the system are correspondingly high. In the present air-water power plant, however, the working temperature is around 100-120°C under low operating pressure, and all the high costs related to the high temperature and pressure would no longer exist. Additionally, in conjunction with hot-water storage systems, the new power plant with a simple structure, 100 MW scale capacity, and low construction costs could operate year-round to attain a high-capacity factor of more than 85%, equal to or above that of fossil-fuel power plants. Therefore, the per kWh capacity costs of the power plant could be much lower than that of PVs plants that normally have a capacity factor of less than 25%. The significant improvement in power capacity along with the high capacity factor and low costs could have a chance to overcome the headwind of worldwide renewable-power buildup and mitigate the constraints of high investment costs and mining resources.
3. A thermal power plant working at a low temperature could be very sensitive to a high ambient temperature in the summer. However, this problem can be resolved by using a chiller to cool the intake air or the air before the compressor system or in the intercooler. Because the temperature reduction of intake air would mainly involve sensible heat with a limited heat extraction out of the air, the use of the chiller with a coefficient of performance (COP) of up 9 to undertake the heat extraction would consume only a limited amount of power. Also, the air-conditioning industry has developed near-zero global warming potential working fluids (Daikin, 2020; Trane, 2022), so the use of a chiller would not cause meaningful greenhouse gas emissions. Therefore, the air-water power plant of this paper can be deployed anywhere in the world and operated at any time.
4. There is normally a tendency to pursue a thermal power plant working at a higher temperature for a higher thermal efficiency according to the Carnot-cycle principle. However, the Carnot-cycle principle only dictates a higher efficiency for the thermal-to-mechanical conversion unit of a power plant, not for the entire power plant. For example, the generally perceived thermal efficiency of around 40% for fossil-fuel power plants is based on the thermal energy received by the thermal-to-mechanical conversion unit. However, if the energy consumption of fuel extraction, processing, and transportation as well as the combustion efficiency and heat losses related to the exhaust combustion gases are included, the overall thermal efficiency for a conventional vapor power plant could be lower than 20%. For a more relevant discussion, consider the performance of the Solar-One project well documented in the book of Stine and Harrigan (1985). The Solar One project is a concentrating solar power (CSP) project based on a central receiver tower of 99 m and more than 1800 heliostat concentrators. The maximum working temperature of the project was above 500°C. The best performance was recorded at the maximum solar input case under the condition of noontime at the summer solstice, resulting in a solar efficiency of 11.25% (Stine and Harrigan, 1985) and a power capacity of about 10 MW. However, the average solar efficiency during a day in the summer could be lower than 10% because at noontime most of the solar flux is in terms of the direct component while in the rest of the day, the diffusion component could be as high as 50% which is unable to be captured by the CSP concentrators. For the present solar power plant of this paper, the solar energy acquisition may be through non-concentrating water-heating solar collectors with a working temperature slightly higher than 100°C, which could attain a collector efficiency of about 60-70%. The thermal to

mechanical conversion efficiency of the present power plant under stable operation based on the storage of hot water could be more than 15%. Therefore, the average solar efficiency could be above 10%. Thus, a high working temperature cannot guarantee the performance advantage of a thermal power system but would incur much higher costs and environmental consequences. Because of the complexity and high costs, CSP installations appear to have almost stalled in recent years, as compared to the growth of PVs. Considering the low costs and 100 MW power capacity scale, non-concentrating solar collectors, hot-water storage, and low-temperature geothermal heat sources, the air-water power plant of this paper could represent a significant advancement in the use of renewable energy sources under environmentally friendly settings.

5. According to EPA (2021), onsite fossil-fuel burning to provide heat for industries and buildings is responsible for 26% of global greenhouse gas emissions. If the fossil fuels are phased out, the heat for industries and buildings may be electrified. If the electricity is generated by PV systems with a 15% electrical efficiency, 1 kWh of electricity would be converted into 1 kWh of heat. In this case, 15% electrical efficiency is equivalent to 15% thermal efficiency. Therefore, in many situations, solar thermal collectors may be favored over PV systems. If a solar thermal collector system is used to provide heat at a temperature over 150ºC with a collector efficiency of only 45%, the solar thermal collector system would still be three times as efficient as the PV system. In the present new power plant, in addition to power production, heat may be supplied from a regenerator or heat/water recovery unit to various users. If the functionality of the heat supply is taken into account, the power plant would be much more valuable. According to Stine and Harrigan (1985), about 50% of the process steam used by industries requires a temperature above 200ºC. Therefore, as part of the strategy to phase out fossil fuels, high-temperature solar collectors and related solar receivers commonly used in CSP could be employed to generate industrial heat at a temperature as high as possible before the use of electricity kicks in.
6. Although low-temperature operations in conjunction with hot-water storage considerations are preferred in this paper, the power plant introduced in this paper in principle would also accommodate high-temperature heat sources including the heat sources related to concentrating solar collectors, combustion, and nuclear reactions, but they are not the subject of this paper.

NOMENCLATURE

C1	The first compressor in Fig. 8
C2	The second compressor in Fig. 8
c_{pa}	Specific heat of dry air (kJ/(kg-ºC))
c_{pv}	Specific heat of vapor (kJ/(kg-ºC))
D	Diameter of the power plant inlet section as shown in Fig. 1 and Fig. 8 (m)
h	Enthalpy (kJ/kg)
h_{a1}	Enthalpy of dry air out of the packing at the top (kJ/kg)
h_{a2}	Enthalpy of dry air into the packing at the bottom (kJ/kg)
h_i	Enthalpy at the turbine inlet (kJ/kg dry-air)
h_o	Enthalpy at the turbine outlet (kJ/kg dry-air)
h_{v1}	Enthalpy of vapor out of the packing at the top (kJ/kg)
h_{v2}	Enthalpy of vapor into the packing at the bottom (kJ/kg)
h_{w1}	Enthalpy of hot water into the packing at the top (kJ/kg)
h_{w2}	Enthalpy of water out of packing at the bottom (kJ/kg)
h_{wr}	Enthalpy of water exiting the regenerator (kJ/kg)
h_{fg}	Latent heat of vaporization (kJ/kg)
$\dot{m}$	Mass for rate or dry air mass flow rate (kg/s)
P	Power plant capacity (MW)
p_{am}	Ambient pressure (bar)
p_b	Pressure at the outlet of the turbine or backpressure (bar)
p_c	Pressure at the inlet of the packing (bar)
p_s	Vapor saturation pressure (bar)
p_t	Total pressure of the moist air or air-vapor mixture in Eqs. (3-4) or the pressure of air-vapor mixture before turbine (bar)
q_{HS}/q	Heat input from heat source in a cycle to the power plant (kJ/kg dry air)
r_{wac}	Ratio of the cooling water flow rate on top of the regenerator to the flow rate of dry air in Fig. 8.
r_{wa1}	Ratio of hot water flow rate at the inlet of the packing to the flow rate of dry air
r_{wa2}	Ratio of water flow rate exiting the packing to the flow rate of dry air
r_{war}	Ratio of water flow rate exiting the regenerator to the flow rate of dry air
t	Temperature (ºC)
t_e	Air-vapor mixture temperature at the exit of the turbine (ºC)
t_{ed}	Air discharge temperature out of power plant in Fig. 8 (ºC)
t_r	Moist air temperature at the outlet of the regenerator (ºC)
t_{re}	Moist air temperature exiting the regenerator in Fig. 8 (ºC)
t_o	Ambient air temperature (ºC)
t_1	Temperature of the air-vapor mixture at the exit of the packing (ºC)
t_2	Temperature of the moist air at the inlet of the packing (ºC)
t_c	The temperature of t he cooling water added to the regenerator in Fig. 8 (ºC)
t_{c1o}	Temperature of the air at the exit of the first compressor (ºC)
t_{c2i}	Temperature of the air at the inlet of the second compressor (ºC)
t_w	Hot-water temperature at the inlet of power plant (ºC)
t_{w1}	Hot water temperature at the inlet of the packing. If water flash is neglected, $t_{w1} = t_w$ (ºC)
t_{w2}	Water temperature at the exit of the packing (ºC)
t_{wr}	Water temperature exiting regenerator (ºC)
V	Average velocity of airflow at the inlet section associated with the diameter D (m/s)
W	Humidity ratio or specific humidity (kg vapor/kg dry air)
W_1	Humidity ratio of the air-vapor mixture at the outlet of the packing (kg vapor/kg dry air)
w_{com}	Work input to compressor system (kJ/kg dry air)
W_e	Humidity ratio of air-vapor mixture at the exit of the turbine (kg vapor/kg dry air)
W_r	Humidity ratio of the moist air at the exit of the regenerator (kg vapor/kg dry air)
W_{re}	Humidity ratio of the moist air exiting the regenerator in Fig. 8 (kg vapor/kg dry air)
W_s	Saturated humidity ratio of the moist air or air-vapor mixture (kg vapor/kg dry air)
W_o	Humidity ratio of the ambient air (kg vapor/kg dry air)
w_{net}	Network output of the power plant per unit dry airflow (kJ/kg dry air)
$w_{chiller}$	Network input to the chiller per unit dry airflow (kJ/kg dry air)
$w_{net,c}$	Corrected network output of the power plant with chiller cooling (kJ/kg dry air)
w_{tur}	Turbine work output (kJ/kg dry air)

Greek Symbols

$\eta_{packing}$	Packing efficiency defined by Eq. (5)
η_c	Isentropic efficiency of the compressor system
η_t	Isentropic efficiency of the turbine

η_{th}	Thermal efficiency of the power plant
$\eta_{th,c}$	Corrected thermal efficiency of the power-plant with chiller cooling
ρ	Air density at the power plant inlet or the inlet of the compressor system (kg/m^3)

Subscripts

1	Top of the packing or the inlet of the turbine
2	Bottom of the packing or the outlet of the compressor system
a	Air
o or am	Ambient condition
v	vapor in the moist air or air-vapor mixture
w	Water
r	Regenerator

REFERENCES

Bathie, W.W., 1996. *Fundamentals of Gas Turbines.* 2nd edition, Wiley, New York.

Cao, Yiding, 2022a, "An Ultimate Solution to Phasing out Fossil Fuels - Part I: Utility-Scale Hot Water Storage (USHWS) for Power Production and Heat Supply," *Frontiers in Heat and Mass Transfer*, Vol. 19. 1. http://dx.doi.org/10.5098/hmt.19.1

Cao, Yiding, 2022b, Air-Water Thermal Power Plants, U.S. Patent Pending, June 19, 2022.

Daikin, 2020. Technology Development to Improve Performance with R-123ze, Retrieved 2022-1-21. https://www.daikinapplied.eu/news-center/the-advantages-of-r1234ze-refrigerant/

EERE – U.S. DOE Energy Efficiency and Renewable Energy, 2022, "Electricity Generation," Retrieved 2022-1-21. https://www.energy.gov/eere/geothermal/electricity-generation#binarycycle

EPA, 2021. Global Greenhouse Gas Emissions Data, Retrieved 2021-12-15. https://www.epa.gov/ghgemissions/global-greenhouse-gas-emissions-data

Evans, P., 2017, Chiller Efficiency How to Calculate, Retrieved 2022-1-21. https://theengineeringmindset.com/chiller-efficiency-calculate/

Hewitt, G.F., Shires, G.L., and Bott, T.R., 1994. *Process Heat Transfer*, Chapters 22 and 23, begell house, Boca Raton.

Hill, G.B. Pring, E.J., and Osborn, P.D., 1990. *Cooling Towers – Principles and Practices*, Butterworth-Heinemann, London.

HVAC HESS, 2022. Chiller Efficiency, Retrieved 2022-1-21. https://www.energy.gov.au/sites/default/files/hvac-factsheet-chiller-efficiency.pdf.

Leeper, S.A., 1981. "Wet Cooling Towers: Rule-of-Thumb Design and Simulation." A Report to Department of Energy, EGG-GTH-5775.

Moran, M.J., Shapiro, H.N., Boettner, D.D., and Bailey, M. B., 2011. *Fundamentals of Engineering Thermodynamics,* 7th Edition, Wiley.

NOAA (National Oceanic and Atmospheric Administration), 2022, Water Cycle, Retrieved 2022-7-8. https://www.noaa.gov/education/resource-collections/freshwater/water-cycle#:~:text=The%20water%20cycle%20shows%20the,form%20of%20rain%20and%20snow.

McQuiston, F.C., Parker, J.D., and Spitler, J.D., 2005, *Heating, Ventilating, and Air Conditioning – Analysis and Design*, 6th Edition, Wiley.

Quoilin, S., Orosz, M., Hemond, H., and Lemort, V., 2011. "Performance and Design Optimization of a Low-Cost Solar Organic Rankine Cycle for Remote Power Generation," *Solar Energy*, Vol. 85, pp. 955–966. http://dx.doi.org/10.1016/j.solener.2011.02.010

Pritchard, P.J. and Leylegian, J.C., 2011. *Fox and McDonald's Introduction to Fluid Mechanics,* 8th Edition, Wiley.

Salameh, Z., 2014. *Renewable Energy System Design*, Chapter 5, pp. 299-371, Academic Press.

Stine, W.B. and Harrigan, R.W., 1985. *Solar energy system and design, Chapter 16: Solar Thermal Projects*, John Wiley, 1985.

Trane, 2022, Sustainable refrigerants: Spotlight on R-454B, Retrieved 2022-1-21. https://www.trane.com/commercial/europe/si/en/about-us/refrigerants-r454b.html

Zengin, G. and Onat, A., 2020, "Experimental and Theoretical Analysis of Mechanical Draft Counterflow Wet Cooling Towers," *Science and Technology for the Built Environment*. http://dx.doi.org/10.1080/23744731.2020.1822084